

Aerosol particles  
over the Aegean Sea

S. Bezantakos et al.

This discussion paper is/has been under review for the journal Atmospheric Chemistry and Physics (ACP). Please refer to the corresponding final paper in ACP if available.

# Chemical composition and hygroscopic properties of aerosol particles over the Aegean Sea

S. Bezantakos<sup>1,2</sup>, K. Barmounis<sup>3</sup>, M. Giamarelou<sup>1</sup>, E. Bossioli<sup>4</sup>, M. Tombrou<sup>1</sup>, N. Mihalopoulos<sup>5</sup>, K. Eleftheriadis<sup>2</sup>, J. Kalogiros<sup>6</sup>, J. D. Allan<sup>7</sup>, A. Bacak<sup>7</sup>, C. J. Percival<sup>7</sup>, H. Coe<sup>7</sup>, and G. Biskos<sup>1,3</sup>

<sup>1</sup>Department of Environment, University of the Aegean, Mytilene 81100, Greece

<sup>2</sup>ERL, Inst. of Nuclear Technology & Radiation Protection, NCSR Demokritos, 15310 Ag. Paraskevi, Attiki, Greece

<sup>3</sup>Faculty of Applied Sciences, Delft University of Technology, Delft 2628-BL, The Netherlands

<sup>4</sup>Department of Physics, National and Kapodistrian University of Athens, Athens 15784, Greece

<sup>5</sup>Department of Chemistry, University of Crete, Heraklion 71003, Greece

<sup>6</sup>Institute of Environmental Research and Sustainable Development, National Observatory of Athens, Athens, Greece

<sup>7</sup>School of Earth, Atmospheric and Environmental Science, The University of Manchester, Manchester, UK

Title Page

Abstract

Introduction

Conclusions

References

Tables

Figures

◀

▶

◀

▶

Back

Close

Full Screen / Esc

Printer-friendly Version

Interactive Discussion



Received: 16 January 2013 – Accepted: 13 February 2013 – Published: 6 March 2013

Correspondence to: G. Biskos (biskos@aegean.gr, g.biskos@tudelft.nl)

Published by Copernicus Publications on behalf of the European Geosciences Union.

**ACPD**

13, 5805–5841, 2013

---

**Aerosol particles  
over the Aegean Sea**

S. Bezantakos et al.

---

Title Page

Abstract

Introduction

Conclusions

References

Tables

Figures

◀

▶

◀

▶

Back

Close

Full Screen / Esc

Printer-friendly Version

Interactive Discussion



## Abstract

The chemical composition and water uptake characteristics of sub-micrometer atmospheric particles in the region of the Aegean Sea were measured between 25 August and 11 September 2011 in the framework of the Aegean-Game campaign. High time-resolution measurements of the chemical composition of the particles were conducted using an airborne compact Time-Of-Flight Aerosol Mass Spectrometer (cTOF-AMS). These measurements involved two flights from the island of Crete to the island of Lemnos and back. A Hygroscopic Tandem Differential Mobility Analyzer (HTDMA) located on the island of Lemnos was used to measure the ability of the particles to take up water. The HTDMA measurements showed that the particles were internally mixed, having hygroscopic growth factors that ranged from 1.00 to 1.59 when exposed to 85 % relative humidity. When the aircraft flew near the ground station on Lemnos, the cTOF-AMS measurements showed that the organic volume fraction of the particles ranged from 43 to 56 %. These measurements corroborate the range of hygroscopic growth factors measured by the HTDMA during that time. Good closure between HTDMA and cTOF-AMS measurements was achieved when assuming that the organic species were hydrophobic and had an average density that corresponds to aged organic species. Using the results from the closure study, the cTOF-AMS measurements were employed to determine a representative aerosol hygroscopic parameter  $\kappa_{\text{mix}}$  for the whole path of the two flights. Calculated  $\kappa_{\text{mix}}$  values ranged from 0.17 to 1.03 during the first flight and from 0.15 to 0.93 during the second flight. Air masses of different origin as determined by back trajectory calculations can explain the spatial variation in the chemical composition and  $\kappa_{\text{mix}}$  values of the particles observed in the region.

## 1 Introduction

Atmospheric aerosol particles affect the global radiative balance of the Earth by directly absorbing and scattering solar radiation (i.e. direct effect; Haywood and Boucher,

ACPD

13, 5805–5841, 2013

## Aerosol particles over the Aegean Sea

S. Bezantakos et al.

Title Page

Abstract

Introduction

Conclusions

References

Tables

Figures

◀

▶

◀

▶

Back

Close

Full Screen / Esc

Printer-friendly Version

Interactive Discussion



**Aerosol particles  
over the Aegean Sea**

S. Bezantakos et al.

Title Page

Abstract

Introduction

Conclusions

References

Tables

Figures

◀

▶

◀

▶

Back

Close

Full Screen / Esc

Printer-friendly Version

Interactive Discussion



2000), and indirectly by acting as Cloud Condensation Nuclei (i.e. indirect effect; Ogren and Charlson, 1992). Scattering and absorption of atmospheric particles strongly depends on their chemical composition, which is often characterised by high variability as a result of the large diversity of their sources and the different physicochemical processes they are involved in during their lifetime (Hallquist et al., 2009). The chemical composition of the particles also defines their hygroscopicity, i.e. their ability to take up water. To predict the hygroscopic behaviour of pure or mixed inorganic particles one can use basic thermodynamic principles (e.g. Clegg et al., 1998). For particles that consist of organic species or mixtures of organic and inorganic compounds, however, existing knowledge does not allow accurate predictions of their hygroscopicity. This limited understanding is one of the greatest uncertainties in determining the role of atmospheric aerosols on climate.

To overcome the complexities involved in associating the chemical composition of atmospheric particles with their hygroscopic behaviour, Petters and Kreidenweis (2007) proposed the use of a single hygroscopic parameter  $\kappa$ . The value of  $\kappa$  is zero for completely insoluble but wettable particles whose water activity is not affected by water adsorbed on their surface. For typical atmospheric soluble-salt particles such as ammonium sulfate or sodium chloride the value of  $\kappa$  is 0.53 and 1.12, respectively, whereas for secondary organic aerosols (SOAs) it typically ranges between 0.0 and 0.2 (Petters and Kreidenweis, 2007). Using the parameter  $\kappa$  and information about the hygroscopic behaviour of the pure chemical species, one can make a good first approximation of the water uptake characteristics of internally mixed particles.

Particles observed in remote areas are typically suspended in the atmosphere long enough to reach an internally mixed state through coagulation and condensation of gaseous species (Heintzenberg, 1989). This is typically the case for the wider area of eastern Mediterranean, and particularly the region over the Aegean Sea, during July and August when the prevailing northern winds (i.e. the Etesians) carry polluted air masses from central Europe, the Balkans (including northern Greece), and the Black Sea (Mihalopoulos et al., 1997; Lelieveld et al., 2002). The polluted air masses blend

with particles emitted from natural sources, e.g. biogenic marine and vegetation emissions, resulting in increased particle concentrations commonly observed in the region (Salisbury et al., 2003).

Although information about the size, the concentration, and the integrated chemical composition of particles found in the southern Aegean has been extensively reported in the literature (e.g. Koulouri et al., 2008; Kalivitis et al., 2008), high-resolution measurements of their hygroscopicity and/or chemical composition has been rather scarce (Pikridas et al., 2010). Engelhart et al. (2011) performed measurements of the integrated hygroscopicity of particles in the submicron range using a Dry-Ambient Aerosol Size Spectrometer (DAASS), whereas Stock et al. (2011) carried out measurements using a Hygroscopic Tandem Differential Mobility Analyzer (HTDMA) system. Both studies were conducted at Finokalia, on the island of Crete, and reported particle hygroscopicities that correspond to mixtures of organic and inorganic compounds.

In this work we report high-resolution chemical composition and hygroscopicity measurements of particles in the atmosphere over the Aegean Sea. Chemical composition measurements of non-refractory fine aerosol particles were conducted using an airborne compact Time-Of-Flight Aerosol Mass Spectrometer (cTOF-AMS) onboard the UK's BAe-146-301 Atmospheric Research Aircraft operated through the Facility for Airborne Atmospheric Measurement (refereed to as the FAAM BAe-146 aircraft from this point onward). Particle hygroscopicity measurements were performed by an HTDMA system located on the island of Lemnos on the North Aegean. Good closure between cTOF-AMS and HTDMA measurements was achieved when the aircraft flew at the vicinity of the ground station. Using the calibration of the closure study, we employ the cTOF-AMS measurements to estimate the hygroscopic parameter  $\kappa_{\text{mix}}$  of the particles across the region between the islands of Crete and Lemnos covered by the aircraft flights.

## Aerosol particles over the Aegean Sea

S. Bezantakos et al.

Title Page

Abstract

Introduction

Conclusions

References

Tables

Figures

◀

▶

◀

▶

Back

Close

Full Screen / Esc

Printer-friendly Version

Interactive Discussion



## 2 Methods

A combination of airborne chemical composition and ground-based hygroscopicity measurements of aerosol particles over the Aegean Sea was performed from 25 August to 10 September 2011. The equipment and the data analysis methods are briefly presented in the following paragraphs.

### 2.1 Experimental

#### 2.1.1 Airborne measurements

The airborne measurements involved a total of three flights from Crete to Lemnos and back with the FAAM BAe146 aircraft (cf. Tombrou et al., 2012). Detailed paths of the flights performed on 1 and 4 September 2011 are shown in Fig. 1. In both flights the aircraft took off from Chania airport, and headed to the east before turning north towards the island of Lemnos. The first flight took place from 09:00 to 13:45 UTC on 1 September. During that flight, the altitude of the aircraft was above 300 m on its way to Lemnos (eastern leg of the flight). To capture the vertical variation of the chemical composition of the particles along this path, the aircraft performed two missed approaches: one halfway towards, and one over the island of Lemnos (Tombrou et al., 2012). The second flight took place from 11:13 to 15:38 UTC on 4 September. During that flight, the altitude of the aircraft along the leg from Crete to Lemnos (i.e. the part over the eastern Aegean Sea) was at lower altitude, almost constantly at 150 m above sea level (a.s.l.). The flight leg from Lemnos to Crete (i.e. the part over the western Aegean Sea) was in general at altitudes above 2300 m during both flights, except for a small period during the second flight when the aircraft flew at 160 m a.s.l. on the southeast of Athens.

The non-refractory submicron chemical composition of the aerosol particles was determined by a cTOF type (Canagaratna et al., 2007; Drewnick et al., 2005) AMS (Aerodyne Research inc.) onboard the aircraft. Details of the airborne cTOF-AMS instrument and the algorithm used for the analysis of the measurements are provided in Morgan

Title Page

Abstract

Introduction

Conclusions

References

Tables

Figures

◀

▶

◀

▶

Back

Close

Full Screen / Esc

Printer-friendly Version

Interactive Discussion



Aerosol particles  
over the Aegean Sea

S. Bezantakos et al.

Title Page

Abstract

Introduction

Conclusions

References

Tables

Figures

◀

▶

◀

▶

Back

Close

Full Screen / Esc

Printer-friendly Version

Interactive Discussion



et al. (2010). In brief, air was sampled through a Rosemount inlet (Foltescu et al., 1995), mounted on the aircraft fuselage. An aerodynamic lens (Wang et al., 2005) was used for focusing the sample particles onto the heated surface maintained at 600 °C. The vapours resulting from volatilising the particles on the heated surface were then ionised using electron impact at 70 eV, and the ion fragments were analysed by a quadruple mass spectrometer for specific ions including  $\text{NH}_4^+$ ,  $\text{Cl}^-$ ,  $\text{NO}_3^-$ ,  $\text{SO}_4^{2-}$  and organics. The cTOF-AMS can measure particles having diameter in the range from 50 to 700 nm (Liu et al., 2007) with a detection limit of ca.  $50 \text{ ng m}^{-3}$ .

### 2.1.2 Ground measurements

The ground-based hygroscopicity measurements were conducted at a station located 420 m a.s.l. in the area of Vigla, on the northwestern part of the island of Lemnos ( $39^\circ 58' \text{ N}$ ,  $25^\circ 04' \text{ E}$ ; cf. Fig. 1). The area is far from any major city and from local anthropogenic sources. A custom-made HTDMA system (Rader and McMurry, 1986) and a commercially available Scanning Mobility Particles Sizer (SMPS, TSI Model 3034; Wang and Flagan, 1989) were used to measure the hygroscopic growth factor and the size distribution of the particles, respectively, at the ground station. For these measurements, ambient air was sampled through a 6-m long copper tube (ID = 26 mm) with a total flow rate of 30.0 lpm at atmospheric conditions. From this flow, 0.3 lpm were sampled by the HTDMA system and 1.0 lpm by the SMPS. A silica-gel diffusion drier was used upstream the two systems in order to maintain the Relative Humidity (RH) of the sampled flow at  $30 \pm 3\%$ . The SMPS system measured the size distribution of the particles having diameters in the range from 10.4 to 469.8 nm, whereas the HTDMA measured the hygroscopicity of the particles having dry diameters from 50 to 170 nm.

The HTDMA system consisted of two Differential Mobility Analyzers (DMAs; Knutson and Whitby, 1975), and a Condensation Particle Counter (CPC, TSI Model 3022A; Stolzenburg and McMurry, 1991). The first DMA (DMA-1, TSI 3080) included a  $^{85}\text{Kr}$  aerosol neutralizer and a closed-loop system for recirculating the sheath flow. The second DMA (DMA-2) employed a custom-made system for the sheath flow recirculation

## Aerosol particles over the Aegean Sea

S. Bezantakos et al.

Title Page

Abstract

Introduction

Conclusions

References

Tables

Figures

◀

▶

◀

▶

Back

Close

Full Screen / Esc

Printer-friendly Version

Interactive Discussion



with an RH controller (cf. Biskos et al., 2006a). For each measurement, the voltage on DMA-1 was adjusted to select dry aerosol particles having mobility diameters from 50 to 170 nm. The quasi-monodisperse particles downstream of DMA-1 were conditioned within a single nafion-tube humidity exchanger (Perma Pure Model MD-110) to a constant RH of 85 %. The size distribution of the humidified particles was then measured by DMA-2 and the CPC. The aerosol and the sheath flows for both DMAs were 0.3 and 3.0 lpm, respectively.

The RH and temperature of the aerosol flow downstream the humidity exchanger and of the sheath flow in DMA-2 were measured by two humidity/temperature sensors (Rotronic Model SC-05). A Proportional-Integral-Derivative (PID) controller was used to control the RH in both streams by adjusting the flow rate of a parallel stream of very high RH (ca. 100 %) on the outer annulus of each nafion-tube humidity exchanger. The overall performance of the HTDMA was tested with ammonium sulfate and sodium chloride particles produced by atomization. The precision of the particle size measurement by the system was less than 1 % and RH variations during the measurements were generally within less than 2 % of the set-point.

## 2.2 Data analysis

### 2.2.1 SMPS measurements

The inversion of the SMPS measurements was performed using the Aerosol Instrument Manager software (AIM, TSI version 6.0), including correction for multiply charged particles. The inverted particle-number size distributions were then analyzed using a curve-fitting algorithm similar to that described in Hussein et al. (2005). This algorithm employed the least squares method to fit the sum of up to three lognormal distributions to the measurements. The first lognormal distribution corresponded to particles having a geometric mean mobility diameter from 10.4 to 25.0 nm (nucleation mode), the second from 25.1 to 90.0 nm (Aitken mode), and third from 90.1 to 500.0 nm (accumulation mode). The geometric standard deviation of each lognormal distribution was allowed

to vary between 1.2 and 2.1. The algorithm starts by fitting a tri-modal lognormal distribution to the measurements, and successively tests the possibility of reducing it to a bi- or to a uni-modal distribution based on the estimated particle-number concentration of each mode, the geometric mean diameter, and the geometric standard deviation of the neighboring modes.

## 2.2.2 HTDMA measurements

The hygroscopic growth factor,  $g$ , determined by the HTDMA measurements is given by

$$g(\text{RH}) = \frac{d_m(\text{RH})}{d_{m,\text{dry}}}, \quad (1)$$

where  $d_m(\text{RH})$  and  $d_{m,\text{dry}}$  are the geometric mean mobility diameters of the sampled particles at the hydrated state (i.e.  $\text{RH} = 85\%$ ) measured by DMA-2 and the CPC, and at the dry state, i.e. the mobility diameter selected by DMA-1, respectively. The RH at the inlet of DMA-1 varied between 27 and 33%, having an average value of 30% during the entire period of the measurements. As a result, the measured growth factor can be more accurately expressed as

$$g(85\%|30\%) = \frac{d_m(85\%)}{d_m(30\%)}. \quad (2)$$

Here  $d_m(30\%)$  is the nominal mobility diameter of the particles selected by DMA-1, and  $d_m(85\%)$  is the mobility diameter measured by DMA-2 and the CPC of the HTDMA system.

Internally mixed monodisperse particles of uniform chemical composition will grow to the same size when subjected to identical RH conditions downstream of DMA-1. Externally mixed particles, on the other hand, can grow to sizes that may or may not be distinguishable in the HTDMA scans. In this case, the size distribution of the humidified

Title Page

Abstract

Introduction

Conclusions

References

Tables

Figures

◀

▶

◀

▶

Back

Close

Full Screen / Esc

Printer-friendly Version

Interactive Discussion



monodisperse particles can exhibit a single mode that is significantly broadened compared to that of the dry sample, or distinct monodisperse modes depending on their hygroscopic variability.

To distinguish between modes that may correspond to different particle populations in a systematic way we employed the TDMAfit algorithm (Stolzenburg and McMurry, 1988) for inverting the HTDMA measurements. The algorithm uses the least squares method to fit Gaussian-shaped transfer functions to the measured response of the system. To locate the peak positions and the associated particle-number concentrations that give the best fit, the algorithm employs a search routine that is based on a number of convergence criteria and constrains. When a chi-square function of the fit residual changes by less than 0.1 % and each of the fitted parameters alters by less than 10 % of its respective estimated uncertainty, the TDMAfit algorithm is considered to have converged to the best fit.

For the analysis of the HTDMA measurements, we assumed that all the particles have a spherical shape when selected by DMA-1, and that particle shrinkage due to the presence of volatile species (e.g. ammonium nitrate) was negligible. Under these assumptions, measured hygroscopic growth factors less than 1.0, comprising ca. 3 % of all the measurements, were excluded.

### 2.2.3 AMS measurements

The cTOF-AMS was calibrated using monodisperse ammonium nitrate particles and the recorded measurements were analyzed using the fragmentation table approach (Allan et al., 2003, 2004) with the modifications introduced by Aiken et al. (2008). Corrections for variations in the composition-dependent collection efficiency were applied according to the parameterization introduced by Middlebrook et al. (2012).

## Aerosol particles over the Aegean Sea

S. Bezantakos et al.

Title Page

Abstract

Introduction

Conclusions

References

Tables

Figures

◀

▶

◀

▶

Back

Close

Full Screen / Esc

Printer-friendly Version

Interactive Discussion



## 2.2.4 Determining hygroscopic growth factors from the AMS measurements

The hygroscopic growth factor of internally mixed particles,  $g_{\text{mix}}$ , can be estimated using the AMS measurements as (Kreidenweis et al., 2008)

$$g_{\text{mix}}(\text{RH}) = \left( 1 + \kappa_{\text{mix}} \left( \frac{\alpha_w}{1 - \alpha_w} \right) \right)^{\frac{1}{3}}, \quad (3)$$

where  $\alpha_w$  is the water activity of the solution droplet, which neglecting the Kelvin effect is equal to  $\text{RH}/100$ , and  $\kappa_{\text{mix}}$  is the hygroscopic parameter of the mixed particles given by

$$\kappa_{\text{mix}} = \sum_i \epsilon_i \kappa_i. \quad (4)$$

Here  $\epsilon_i = V_{\text{si}}/V_{\text{s}}$  and  $\kappa_i$  are the volume fraction and the hygroscopic parameter of the  $i$ th chemical species of the particles, with  $V_{\text{si}}$  being the volume occupied by that species and  $V_{\text{s}}$  the dry volume of the particle.

To estimate the volume fractions of each species of the particles from the cTOF-AMS mass measurements we first determined the molar fractions of the ions and then those of the chemical compounds comprising the particles using the ion pairing algorithm proposed by Pilinis et al. (1987), and later simplified by Gysel et al. (2007). In this simplified algorithm, by setting the fraction of nitric acid to zero, the molar fraction of ammonium nitrate is equal to the molar fraction of nitrate ions. The rest of the ammonium ions are assigned to the sulfate ions, and depending on the ammonium to sulfate ratio, the molar fractions of sulfuric acid, ammonium bisulfate and ammonium sulfate are determined. To convert the mole fractions to volume fraction we then use the bulk densities for every chemical species as summarized in Table 1 (Duplissy et al., 2011). The respective hygroscopic parameters are also shown in Table 1 (Petters and Kreidenweis, 2007). For the organic compounds commonly present in atmospheric particles the density,  $\rho_{\text{org}}$ , and hygroscopic parameter,  $\kappa_{\text{org}}$ , can vary from 1200 to 1700  $\text{kgm}^{-3}$  (Hallquist et al., 2009), and from 0.0 to 0.2 (Petters and Kreidenweis, 2007), respectively.

Title Page

Abstract

Introduction

Conclusions

References

Tables

Figures

◀

▶

◀

▶

Back

Close

Full Screen / Esc

Printer-friendly Version

Interactive Discussion



### 3 Results and discussion

The prevailing synoptic conditions during the entire period of the measurements correspond mainly to north easterlies surface winds over the Aegean Sea being associated with a large-scale surface anticyclone. From 30 August to 3 September, however, the wind speeds were substantially lower with northwesterly directions. In particular, during the first flight (1 September), a large-scale surface anticyclone prevailed over southeastern Europe, producing fair weather conditions and a moderate flow from the north-east sector over the Aegean Sea. During the second flight (4 September), the low pressure pattern that prevailed over the southeastern Europe, in combination with the anticyclone over Balkans, resulted in a strong channeled surface-wind flow over the Aegean Sea. Average wind speeds of up to  $20 \text{ ms}^{-1}$  were measured at altitudes 150 m a.s.l., but diminished above 4500 m. When the aircraft flew at the vicinity of the station on Lemnos the surface winds were from southwest direction and lower than  $5 \text{ ms}^{-1}$  during the first flight, and from northeast directions with speeds ranging from 9.5 to  $13 \text{ ms}^{-1}$  during the second flight. The surface temperature and RH at the ground station on Lemnos during the two missed approaches were 28 and  $21^\circ\text{C}$ , and 45 and 75 %, respectively. For the entire period of the measurements, the surface temperature and the RH at the ground station on Lemnos ranged from 17.7 to  $29.6^\circ\text{C}$  and from 16 to 87 %, respectively.

#### 3.1 Measurements in the atmosphere over the ground station

As described in Sect. 2.1, the size distributions and the hygroscopicities of the particles were continuously measured at the ground station during the entire period of the campaign. During each flight, the FAAM BAe146 aircraft flew at the vicinity of the ground station (i.e.  $\pm 300$  m above or below the station and within a radius of 30 km) for approximately 10 to 15 min. The measurements performed by the airborne cTOF-AMS during these two time windows were used to check the closure between hygroscopicity and

Title Page

Abstract

Introduction

Conclusions

References

Tables

Figures

◀

▶

◀

▶

Back

Close

Full Screen / Esc

Printer-friendly Version

Interactive Discussion



chemical composition measurements. The following paragraphs provide an overview of the ground-based measurements and the closure study.

### 3.1.1 Particle size distributions

The diurnal variation of the total number concentration of particles in the nucleation, the Aitken, and the accumulation mode measured by the SMPS for all the days of the experiment are shown in Fig. 2. The total number concentration of the particles having diameter from 10.4 to 469.8 nm varied from ca.  $2 \times 10^2$  to  $1.4 \times 10^4$  particles  $\text{cm}^{-3}$  with median value of  $1.9 \times 10^3$ . Almost 72.1 % of the samples had bi-modal distributions, whereas 14.2 % and 13.7 % of them exhibited uni-modal and tri-modal distributions, respectively. Particles in the Aitken mode show the highest variance compared to particles in the two other modes. The total particle number concentration in the nucleation mode varied from zero to  $1.3 \times 10^4$  particles  $\text{cm}^{-3}$ , with a median value of  $4 \times 10^2$ , in the Aitken mode from zero to  $1.1 \times 10^4$  particles  $\text{cm}^{-3}$ , with a median value of  $8.8 \times 10^2$ , and in the accumulation mode from  $5.4 \times 10^1$  to  $7.3 \times 10^3$  particles  $\text{cm}^{-3}$ , with a median value of  $8.8 \times 10^2$ . The majority of the particles were observed in the Aitken and the accumulation mode during the entire period of the measurements. In general, the mean concentration of the nucleation-mode particles gradually decreased from midnight to midday, increased from noon to ca. 17:00–18:00, and decreased again until the end of the day. A similar variation is observed for the accumulation-mode particles, whereas the diurnal variation of the Aitken-mode particles is more stable.

Nucleation events occurred on 23 and 24 August, as well as on 10 September (data not shown in Fig. 2). During those days the concentration of nucleation-mode particles started to increase around 10:00, exhibited a peak between 12:00 and 15:00 and reduced significantly after 16:00. On these days the concentration of Aitken-mode particles increased gradually throughout the day, as a result of the growth of the nucleation mode particles. The concentration of accumulation-mode particles was overall more stable as compared to the other two modes.

## Aerosol particles over the Aegean Sea

S. Bezantakos et al.

Title Page

Abstract

Introduction

Conclusions

References

Tables

Figures

◀

▶

◀

▶

Back

Close

Full Screen / Esc

Printer-friendly Version

Interactive Discussion



### 3.1.2 Particle hygroscopicity

Characteristic raw measurements from the ground-based HTDMA are shown in Fig. 3. The recorded size distributions correspond to particles having dry mobility diameters (i.e. diameters selected by DMA-1) of 70, 90, and 150 nm, after being exposed to 85 % RH. The respective hygroscopic growth factors  $g(85\%/30\%)$  of those samples are 1.22, 1.22, and 1.21. In almost all the HTDMA measurements, the geometric standard deviation of the size distribution of the humidified particles was similar to that of the dry ones, indicating that the samples were internally mixed. This is typical in remote areas with no major local anthropogenic particle sources.

Figure 4 shows the hygroscopic growth factors  $g(85\%/30\%)$  measured by the HTDMA during the entire period of the campaign. The measurements are grouped in three different classes depending on the dry mobility diameters selected by DMA-1: green circles correspond to measurements of particles having dry mobility diameter from 50 to 80 nm, red squares from 80 to 100 nm, and blue diamonds from 100 to 170 nm (note that in general the dry diameter was selected to be close to the peak of the most dominant mode of the particle size distribution as measured by the SMPS). The average growth factor for all particle sizes was 1.20, having a minimum value of 1.00 and a maximum of 1.59. Periods with particles of high (from 25 to 30 August), low (from 30 August to 2 September) and moderate (from 2 to 9 September) variation in the growth factor can be identified in the HTDMA measurements. Differences in this variation are well correlated with the variability of the origin of the air masses arriving at the station. During the days with low variation in particle hygroscopicity, the air-masses reaching the station had almost the same origin (i.e. the Black Sea) as indicated in Fig. S1.

Although the selected dry diameters correspond to different periods during the campaign, they exhibit very similar growth factors when comparing nearby measurements. Considering also that the variability and the average growth factors corresponding to particles having different dry diameters are also very similar, suggests that there is no

Title Page

Abstract

Introduction

Conclusions

References

Tables

Figures

◀

▶

◀

▶

Back

Close

Full Screen / Esc

Printer-friendly Version

Interactive Discussion



noticeable variation of chemical composition as a function of particles size. It should also be pointed out that the total range of selected dry particles was from 50 to 170 nm, within which the contribution of the Kelvin effect to the hygroscopic growth of the particles is negligible (Biskos et al., 2006b; Park et al., 2009).

5 The average hygroscopic growth factor measured in this work is ca. 12 % lower compared to those reported by Stock et al. (2011) who also used an HTDMA system at Finokalia, on the island of Crete, from 12 August to 20 October 2005. The hygroscopic growth factors of particles having dry diameters 50, 80, and 150 nm observed during that study ranged from 1.12 (nearly hydrophobic particles) to 1.59 (more hygroscopic particles). Considering that those HTDMA measurements were conducted at 90 % RH, using the  $\kappa$ -Köhler theory (i.e. Eqs. 3 and 4) we calculate the corresponding growth factors at 85 % RH to be in the range from 1.08 to 1.43. Although this range is similar to that observed in our study, the occurrence frequency of the more hygroscopic particles reported by Stock et al. (2011) was significantly higher (of the order of 84 to 90 %) compared to our study (i.e. ca. 35 %).

### 3.1.3 Particle chemical composition and hygroscopicity

Figure 5 shows the chemical composition of the atmospheric particles when the aircraft was flying within a 30-km radius from the ground station and between 100 and 700 m altitude (i.e. ca.  $\pm 300$  m from the altitude of the ground station). The reported volume fractions are estimated by applying the ion pairing algorithm to the cTOF-AMS measurements (cf. Sect. 2.2.4). The organic species comprised almost 50 % of the total particle dry volume, whereas ammonium sulfate and ammonium bisulfate accounted for the rest. Although the volume fraction of the organic species was almost the same during both days, the inorganic fraction of the particles was slightly more acidic during the flight on 4 September (Fig. 5b).

25 Considering that on 1 and 4 September the chemical composition of the particles did not show high variability with size (data not shown), the cTOF-AMS measurements can be considered as representative for the entire particle size range and can be used to

Title Page

Abstract

Introduction

Conclusions

References

Tables

Figures

◀

▶

◀

▶

Back

Close

Full Screen / Esc

Printer-friendly Version

Interactive Discussion



Aerosol particles  
over the Aegean Sea

S. Bezantakos et al.

predict the hygroscopic growth of the particles using the  $\kappa$ -Köhler theory. The comparison between predicted (i.e. using Eqs. (3) and (4) and the cTOF-AMS measurements) and measured (i.e. using Eq. (2) and the HTDMA measurements) hygroscopic growth factors is shown in Fig. 6. The particles measured by the HTDMA had dry mobility diameters of 100 nm. To account for the fact that the relative humidity of the dry sample was 30 %, and therefore the particles entering the HTDMA may have already had some water due to their acidity (cf. Biskos et al., 2009; Engelhart et al., 2011) and/or their organic content (cf. Marcolli et al., 2004), we calculate the absolute growth factor at 85 % RH as

$$g(85\%) = \frac{d_m(85\%)}{d_{m,dry}} = \frac{d_m(30\%)}{d_{m,dry}} \times \frac{d_m(85\%)}{d_m(30\%)} = g(30\%) \times g(85\%|30\%). \quad (5)$$

Here  $g(85\%|30\%)$  is the measured growth factor (cf. Eq. 2), and  $g(30\%)$  is the growth factor of the particles entering the HTDMA at 30 % RH. The latter is estimated using the  $\kappa$ -Köhler theory and the composition measurements provided by the cTOF-AMS. The estimated  $g(30\%)$  values varied from 1.03 to 1.06 during the specific measurements.

For the predicted growth factors shown in Fig. 6 we assumed that the organic fraction of the particles was hydrophobic (i.e. that  $\kappa_{org}$  was equal to zero), having an average density,  $\rho_{org}$ , of  $1270 \text{ kg m}^{-3}$  which is typical of aged organic species (Cross et al., 2007). Using these parameters, the comparison between hygroscopic growth factors measured by the HTDMA system and those predicted using the  $\kappa$ -Köhler theory and the cTOF-AMS measurements shows good agreement when the aircraft was flying in the vicinity of the ground station. The predicted hygroscopic growth factors on 1 September are ca. 3 % higher compared to those on 4 September, as a result of the slightly higher acidity of the inorganic fraction of the particles (cf. Fig. 6). The hygroscopic growth factors measured by the HTDMA on other hand are lower on the 1 September compared to those on 4 September. In either case, the maximum difference between predicted and measured growth factors was below 5 %, which is well within our experimental uncertainty.

Title Page

Abstract

Introduction

Conclusions

References

Tables

Figures

◀

▶

◀

▶

Back

Close

Full Screen / Esc

Printer-friendly Version

Interactive Discussion



Aerosol particles  
over the Aegean Sea

S. Bezantakos et al.

Title Page

Abstract

Introduction

Conclusions

References

Tables

Figures

◀

▶

◀

▶

Back

Close

Full Screen / Esc

Printer-friendly Version

Interactive Discussion



We further provide a sensitivity analysis to investigate the range of possible  $\kappa_{\text{org}}$  and  $\rho_{\text{org}}$  values that would warrant an agreement between measured and predicted hygroscopic growth factors within experimental uncertainty. Raising either the hygroscopic parameter or the density of the organic species results in an increase of the predicted hygroscopic growth factor. Keeping the average organic density at  $1270 \text{ kg m}^{-3}$ , an increase of 5 % in the predicted growth factor would require an increase of  $\kappa_{\text{org}}$  from zero to ca. 0.1. In a similar fashion, increasing  $\rho_{\text{org}}$  by 34 % (i.e. from  $1270$  to  $1700 \text{ kg m}^{-3}$ , which is the maximum density typically associated with organic compounds present on atmospheric particles), while maintaining the value of  $\kappa_{\text{org}}$  to zero, would result in an increase of the predicted hygroscopic growth factor by 3 %. The hygroscopic growth factor is evidently more sensitive in changes of  $\rho_{\text{org}}$  than in changes of  $\kappa_{\text{org}}$ , and a number of combinations would give a good agreement between measurements and predictions. However, given that good closure between cTOF-AMS and HTDMA is achieved when relatively low  $\kappa_{\text{org}}$  and  $\rho_{\text{org}}$  values are used, indicates that the organic fraction of the particles is hydrophobic and of low density.

## 3.2 Measurements in the atmosphere over the Aegean Sea

As already discussed in the preceding sections, the ability of atmospheric particles to take up water strongly depends on their chemical composition. In the paragraphs that follow we provide an overview of the cTOF-AMS chemical composition measurements conducted over the Aegean Sea during the two flights of the campaign, and employ them to predict the representative hygroscopic parameter of the particles using the  $\kappa$ -Köhler theory.

### 3.2.1 Particle chemical composition

The volume fractions of the compounds comprising the particles observed during the entire flights on 1 and 4 September are shown in Figs. 7 and 8, respectively.

**Aerosol particles  
over the Aegean Sea**

S. Bezantakos et al.

During the flight on 1 September (data shown in Fig. 7) the volume fraction of sulfuric acid, ammonium bisulfate, and ammonium sulfate range from zero to 0.86, with a median value of zero, from zero to 0.66, with a median value of 0.22, and from zero to 1.00, with a median value of 0.31, respectively. In two of the four vertical paths of the flight (i.e. above the central Aegean Sea, and above Lemnos), the acidity of the particles appears to increase with increasing height, indicating that the concentration of ammonia is very low at high altitudes as had been observed in other regions (e.g. Spengler et al., 1990). The volume fraction of ammonium bisulfate is almost zero at lower altitudes, rising to 0.5 at 2500 m a.s.l. This pattern is inverted in the two vertical paths above Crete. The volume fractions of ammonium bisulfate in this case appear to be high at lower altitudes (< 700 m a.s.l.), and, with the exception of a couple of points (one around 2000 and one 3700 m a.s.l.), to decrease with increasing height. In all cases, the concentration of  $\text{H}_2\text{SO}_4$  is almost zero for the entire flight, with the exception of a few measurements above 4000 m a.s.l. over Crete.

As shown by back trajectory calculations (cf. Fig. S2), low-altitude air masses arriving over the north or central Aegean Sea originate from eastern Europe and the wider Black Sea region. These air masses appear to carry particles of very low acidity as shown in Fig. 7. The low-altitude air masses arriving over Crete on the other hand originate either from the marine environment or from the mainland, but in both cases they pass over the wider Athens region. This can explain the high acidity of the particles observed at lower altitudes in that area. Acidic particles formed or directly emitted from anthropogenic activities in the region of Athens, travel over the central Aegean Sea towards Crete. The acidity of these particles does not change significantly during advection as a result of the low concentrations of ammonia over the marine environment (Clarisse et al., 2009). Acidic particles coming from eastern Europe on the other hand (i.e. those arriving over the north Aegean Sea) have a greater chance of being neutralized due to the higher concentration of ammonia over the mainland.

The organic volume fraction of the particles observed during the first flight range from zero to 0.74, with a median value of 0.46. The measurements show similar vertical

[Title Page](#)[Abstract](#)[Introduction](#)[Conclusions](#)[References](#)[Tables](#)[Figures](#)[◀](#)[▶](#)[◀](#)[▶](#)[Back](#)[Close](#)[Full Screen / Esc](#)[Printer-friendly Version](#)[Interactive Discussion](#)

**Aerosol particles  
over the Aegean Sea**

S. Bezantakos et al.

5 variability during all four vertical parts of the flight: they start with low values at the lower altitudes, they increase at intermediated heights and decrease again at even higher levels. The height of the layers with particles of high organic fractions differ from place to place, with the highest layer observed over the central Aegean Sea. Considering that the air masses arriving over Lemnos and the central Aegean Sea during the respective missed approaches have passed over cities and rural areas and that their origin is similar (i.e. from eastern Europe), the organic fraction of the particles can be either biogenic or anthropogenic.

10 The chemical composition of the particles observed during the flight on 4 September is shown in Fig. 8. During that flight the aircraft flew at lower altitudes from Crete to Lemnos (eastern leg of the flight) and at higher altitudes from Lemnos to Crete (western leg of the flight). Three of the four vertical parts of the flight in this case ended at substantially higher altitudes (ca. 4000 m a.s.l.) compared to those of the first one. The vertical part of the flight over the central Aegean Sea was limited to ca. 1000 m. The volume fraction of sulfuric acid, ammonium bisulfate, and ammonium sulfate ranged from zero to 0.79, with a median value of zero, from zero to 0.69 with a median value of 0.10, and from zero to 0.97, with a median value of 0.35, respectively. Similarly to the measurements recorded during the first flight, particle acidity increased with increasing altitude. In this case, however, the particles observed at ca. 2500 m a.s.l. (i.e. similar to the altitude of the eastern leg of the first flight) were even more acidic, having a  $\text{H}_2\text{SO}_4$  volume fraction that reached values as high as ca. 0.4. High volume fractions of  $\text{NH}_4\text{HSO}_4$  are observed at a layer between 1000 and 2000 m a.s.l. over the west/northwest of Crete.

25 The respective fractions for the organic compounds of the particles during the second flight ranged from 0.03 to 0.84, with a median value of 0.48. An increasing particle organic content is observed with increasing altitude, having median volume fractions of 0.44 and 0.54 for altitudes below and above 2000 m, respectively. Compared to the first flight, the vertical distributions exhibit a higher uniformity among the vertical paths of the flight. The uniformity of the vertical variation of the organic fraction of the particles

[Title Page](#)[Abstract](#)[Introduction](#)[Conclusions](#)[References](#)[Tables](#)[Figures](#)[◀](#)[▶](#)[◀](#)[▶](#)[Back](#)[Close](#)[Full Screen / Esc](#)[Printer-friendly Version](#)[Interactive Discussion](#)

is also higher compared to that of the first flight. This can be explained by the fact that the air masses arriving in many regions over the study area all originate from central/western Europe and follow similar paths (cf. Fig. S3).

### 3.2.2 Particle hygroscopicity

Using the chemical composition measurements discussed above, we calculate the aerosol hygroscopic parameter  $\kappa_{\text{mix}}$  (Eq. 4) for the entire path of the two flights as shown in Fig. 9. For these calculations we used the hygroscopic parameter and the density of the organic fraction of the particles derived from the closure study (i.e.  $\kappa_{\text{org}} = 0$  and  $\rho_{\text{org}} = 1270 \text{ kg m}^{-3}$ ; cf. Sect. 3.1.3 and Fig. 6), and assumed that all the samples were internally mixed. For the flight on 1 September (Fig. 9a) the hygroscopic parameter ranged from 0.17 to 1.03, with a median value of 0.28. A striking observation here is that the hygroscopic parameter of the particles observed along the eastern leg of the flight is substantially higher compared to that along the western leg at 2500 m a.s.l. This can be explained by differences in the acidity and the organic fraction of the particles in the two paths. Along the eastern leg of the flight the organic volume fraction is smaller, whereas the acidity is higher compared to those in the western leg. The vertical variation of the hygroscopic parameter of the particles also follows the variation of their acidity. An interesting observation here is that the hygroscopicity of the particles observed at low altitudes over Crete is higher compared to those observed over the central Aegean Sea and Lemnos at similar heights. This difference can be explained by the influence of air masses arriving from the wider Athens region as described in Sect. 3.2.1. The highest  $\kappa_{\text{mix}}$  values during the first flight were calculated north of the island of Crete at 4000 m altitude, where the particles were highly acidic.

The hygroscopic parameters predicted for the flight on 4 September are shown in Fig. 9b. In this case, the calculated  $\kappa_{\text{mix}}$  values exhibited a variability that is smaller (from 0.15 to 0.93), and a median value (ca. 0.30) that is comparable to that calculated for the first flight. At altitudes above 2000 m (western leg of the flight) the particles exhibit a relatively high hygroscopicity with many points having  $\kappa_{\text{mix}}$  values greater

## Aerosol particles over the Aegean Sea

S. Bezantakos et al.

Title Page

Abstract

Introduction

Conclusions

References

Tables

Figures

◀

▶

◀

▶

Back

Close

Full Screen / Esc

Printer-friendly Version

Interactive Discussion



than 0.8. For other points, however, the hygroscopicity of the particles observed at this height is at moderate levels due to their high organic fraction. At lower altitudes (eastern leg of the flight) the particles have a more uniform  $\kappa_{\text{mix}}$  values with a median of ca. 0.3. This can be well explained by the low acidity (i.e. the inorganic fraction of the particles is mostly ammonium sulfate) and relatively low organic volume fractions of the particles. For the vertical profile over the western/northwestern part of Crete the hygroscopicity of the particles appears to increase with increasing altitude as a result of their increasing acidity (i.e. the volume fraction of ammonium bisulfate increases with increasing altitude as shown in Fig. 8b).

## 4 Conclusions

Measurements of the chemical composition and hygroscopicity of atmospheric particles were conducted in the region of the Aegean Sea using a cTOF-AMS onboard the FAAM BAe-146 aircraft, and a ground-based HTDMA system located on a remote station on the island of Lemnos. The HTDMA measurements showed that the mean hygroscopic growth factor of particles having dry diameters from 50 to 170 nm was ca. 1.2, and that the aerosol samples were internally mixed during the entire period of the campaign. Good closure between cTOF-AMS and HTDMA measurements was achieved when the aircraft flew in the vicinity of the ground station. For the closure we assumed that the organic fraction of the particles was totally hydrophobic (i.e.  $\kappa_{\text{org}} = 0$ ), having a density of  $1270 \text{ kg m}^{-3}$  that is representative of aged organic species.

The particles observed over the wider region of the Aegean Sea during the two flights exhibited high variability in their acidity and organic volume fraction, which can be attributed to differences in the origin of the air masses arriving in the region. During the first flight, the air masses arriving over the north and central Aegean Sea had origins ranging from eastern Europe, the Black Sea, and the Balkans, while those arriving over Crete had passed near the city of Athens, transferring anthropogenic emissions. During the second flight, air masses originated mainly from western and central Europe and

Title Page

Abstract

Introduction

Conclusions

References

Tables

Figures

◀

▶

◀

▶

Back

Close

Full Screen / Esc

Printer-friendly Version

Interactive Discussion



**Aerosol particles  
over the Aegean Sea**

S. Bezantakos et al.

Title Page

Abstract

Introduction

Conclusions

References

Tables

Figures

◀

▶

◀

▶

Back

Close

Full Screen / Esc

Printer-friendly Version

Interactive Discussion



the wind patterns were more uniform and representative of the summer period in the region. For both flights we observed that the organic species accounted for almost 50 % of the volume of the particles, and that their acidity increased with increasing altitude. Higher spatial uniformity of the chemical composition of the particles was observed during the second flight as a result of the low variability in the origin and the paths of the air masses arriving in the region. The acidity of the particles observed during that flight was significantly high at high altitudes, exhibiting H<sub>2</sub>SO<sub>4</sub> volume fractions of up to 0.4.

Assuming that the organic fraction of the particles was hydrophobic having a density of 1270 kg m<sup>-3</sup> (as indicated by the closure study performed when the aircraft flew in the vicinity of the ground station), the cTOF-AMS chemical composition measurements were used to estimate the aerosol single hygroscopic parameter  $\kappa_{\text{mix}}$  for the entire path of the flights. Although the median hygroscopic parameter was very similar for both flights (i.e. ca. 0.30), its spatial variability was higher during the first flight. This can be explained by the high diversity in the origin of the air masses arriving in the study region and the contribution of polluted air from the wider Athens area over the southern Aegean Sea during that flight. Despite the difference in the variability of the hygroscopic parameter of the particles observed in the two flights, overall it increased with increasing altitude as a result of the higher acidity of the particles.

**Supplementary material related to this article is available online at:**  
[http://www.atmos-chem-phys-discuss.net/13/5805/2013/  
acpd-13-5805-2013-supplement.pdf](http://www.atmos-chem-phys-discuss.net/13/5805/2013/acpd-13-5805-2013-supplement.pdf).

*Acknowledgements.* The airborne measurements reported in this work have been supported by the EUFAR (227159) EC Grant Agreement under the Aegean-Game-2 project. Airborne data was obtained using the BAe-146-301 Atmospheric Research Aircraft (ARA) flown by Directflight Ltd and managed by the Facility for Airborne Atmospheric Measurements (FAAM), which is a joint entity of the Natural Environment Research Council (NERC) and the Met Office.

The ground measurements have been co-financed by the European Union (European Social Fund – ESF) and Greek national funds through the Operational Program “Education and Lifelong Learning” of the National Strategic Reference Framework (NSRF) – Research Funding Program: Heracleitus II. Investing in knowledge society through the European Social Fund.

## 5 References

- Aiken, A. C., Decarlo, P. F., Kroll, J. H., Worsnop, D. R., Huffman, J. A., Docherty, K. S., Ulbrich, I. M., Mohr, C., Kimmel, J. R., Sueper, D., Sun, Y., Zhang, Q., Trimborn, A., Northway, M., Ziemann, P. J., Canagaratna, M. R., Onasch, T. B., Alfarra, M. R., Prévôt, A. S.H., Dommen, J., Duplissy, J., Metzger, A., Baltensperger, U., and Jimenez, J. L.: O/C and OM/OC ratios of primary, secondary, and ambient organic aerosols with high-resolution time-of-flight aerosol mass spectrometry, *Environ. Sci. Technol.*, 42, 4478–4485, 2008. 5814
- Allan, J. D., Jimenez, J. L., Williams, P. I., Alfarra, M. R., Bower, K. N., Jayne, J. T., Coe, H., and Worsnop, D. R.: Quantitative sampling using an aerodyne aerosol mass spectrometer – 1. Techniques of data interpretation and error analysis, *J. Geophys. Res.-Atmos.*, 108, 4090, doi:10.1029/2002JD002358, 2003. 5814
- Allan, J. D., Coe, H., Bower, K. N., Alfarra, M. R., Delia, A. E., Jimenez, J. L., Middlebrook, A. M., Drewnick, F., Onasch, T. B., Canagaratna, M. R., Jayne, J. T., and Worsnop, D. R.: A generalised method for the extraction of chemically resolved mass spectra from aerodyne aerosol mass spectrometer data, *J. Aerosol Sci.*, 35, 909–922, 2004. 5814
- Biskos, G., Paulsen, D., Russell, L. M., Buseck, P. R., and Martin, S. T.: Prompt deliquescence and efflorescence of aerosol nanoparticles, *Atmos. Chem. Phys.*, 6, 4633–4642, doi:10.5194/acp-6-4633-2006, 2006a. 5812
- Biskos, G., Russel, L. M., Buseck, P. R., and Martin, S. T.: Nanosize effect on the hygroscopic growth factor of aerosol particles, *Geophys. Res. Lett.*, 33, L07801, doi:10.1029/2005GL025199, 2006b. 5819
- Biskos, G., Buseck, P. R., and Martin, S. T.: Hygroscopic growth of nucleation-mode acidic sulfate particles, *J. Aerosol Sci.*, 40, 338–347, 2009. 5820
- Canagaratna, M. R., Jayne, J. T., Jimenez, J. L., Allan, J. D., Alfarra, M. R., Zhang, Q., Onasch, T. B., Drewnick, F., Coe, H., Middlebrook, A., Delia, A., and Williams, L. R., Trimborn, A. M., Northway, M. J., DeCarlo, P. F., Kolb, C. E., Davidovits, P., and Worsnop, D. R.: Chemical and

## Aerosol particles over the Aegean Sea

S. Bezantakos et al.

Title Page

Abstract

Introduction

Conclusions

References

Tables

Figures

◀

▶

◀

▶

Back

Close

Full Screen / Esc

Printer-friendly Version

Interactive Discussion



Aerosol particles  
over the Aegean Sea

S. Bezantakos et al.

Title Page

Abstract

Introduction

Conclusions

References

Tables

Figures

◀

▶

◀

▶

Back

Close

Full Screen / Esc

Printer-friendly Version

Interactive Discussion



microphysical characterization of ambient aerosols with the aerodyne aerosol mass spectrometer, *Mass Spectrom. Rev.*, 26, 185–222, 2007. 5810

Clarisse, L., Clerbaux, C., Dentener, F., Hurtmans, D., and Coheur, P.-F.: Global ammonia distribution derived from infrared satellite observations, *Nature Geosci.*, 2, 479–483, 2009. 5822

Clegg, S. L., Brimblecombe, P., and Wexler, A. S.: Thermodynamic model of the system  $\text{H}^+$ - $\text{NH}_4^+$ - $\text{SO}_4^{2-}$ - $\text{NO}_3$ - $\text{H}_2\text{O}$  at tropospheric temperatures, *J. Phys. Chem. A*, 102, 2137–2154, 1998. 5808

Cross, E. S., Slowik, J. G., Davidovits, P., Allan, J. D., Worsnop, D. R., Jayne, J. T., Lewis, D. K., Canagaratna, M., and Onasch, T. B.: Laboratory and ambient particle density determinations using light scattering in conjunction with aerosol mass spectrometry, *Aerosol Sci. Tech.*, 41, 343–359, 2007. 5820

Drewnick, F., Hings, S. S., DeCarlo, P., Jayne, J. T., Gonin, M., Fuhrer, K., Weimer, S., Jimenez, J. L., Demerjian, K. L., Borrmann, S., and Worsnop, D. R.: A new time-of-flight aerosol mass spectrometer (TOF-AMS)-instrument description and first field deployment, *Aerosol Sci. Tech.*, 39, 637–658, 2005. 5810

Duplissy, J., DeCarlo, P. F., Dommen, J., Alfarra, M. R., Metzger, A., Barmpadimos, I., Prevot, A. S. H., Weingartner, E., Tritscher, T., Gysel, M., Aiken, A. C., Jimenez, J. L., Canagaratna, M. R., Worsnop, D. R., Collins, D. R., Tomlinson, J., and Baltensperger, U.: Relating hygroscopicity and composition of organic aerosol particulate matter, *Atmos. Chem. Phys.*, 11, 1155–1165, doi:10.5194/acp-11-1155-2011, 2011. 5815

Engelhart, G. J., Hildebrandt, L., Kostenidou, E., Mihalopoulos, N., Donahue, N. M., and Pandis, S. N.: Water content of aged aerosol, *Atmos. Chem. Phys.*, 11, 911–920, doi:10.5194/acp-11-911-2011, 2011. 5809, 5820

Foltescu, V. L., Selin, E., and Below, M.: Corrections for particle losses and sizing errors during aircraft aerosol sampling using a rosemount inlet and the pms las-x, *Atmos. Environ.*, 29, 449–453, 1995. 5811

Gysel, M., Crosier, J., Topping, D. O., Whitehead, J. D., Bower, K. N., Cubison, M. J., Williams, P. I., Flynn, M. J., McFiggans, G. B., and Coe, H.: Closure study between chemical composition and hygroscopic growth of aerosol particles during TORCH2, *Atmos. Chem. Phys.*, 7, 6131–6144, doi:10.5194/acp-7-6131-2007, 2007. 5815

Hallquist, M., Wenger, J. C., Baltensperger, U., Rudich, Y., Simpson, D., Claeys, M., Dommen, J., Donahue, N. M., George, C., Goldstein, A. H., Hamilton, J. F., Herrmann, H., Hoffmann, T., Iinuma, Y., Jang, M., Jenkin, M. E., Jimenez, J. L., Kiendler-Scharr, A., Maen-

Aerosol particles  
over the Aegean Sea

S. Bezantakos et al.

Title Page

Abstract

Introduction

Conclusions

References

Tables

Figures

◀

▶

◀

▶

Back

Close

Full Screen / Esc

Printer-friendly Version

Interactive Discussion



haut, W., McFiggans, G., Mentel, Th. F., Monod, A., Prévôt, A. S. H., Seinfeld, J. H., Surratt, J. D., Szmigielski, R., and Wildt, J.: The formation, properties and impact of secondary organic aerosol: current and emerging issues, *Atmos. Chem. Phys.*, 9, 5155–5236, doi:10.5194/acp-9-5155-2009, 2009. 5808, 5815

5 Haywood, J. and Boucher, O.: Estimates of the direct and indirect radiative forcing due to tropospheric aerosols: a review, *Rev. Geophys.*, 38, 513–543, 2000. 5808

Heintzenberg J.: Fine particles in the global troposphere. a review, *Tellus B*, 41, 149–160, 1989. 5808

10 Hussein, T., Maso, M. D., Petäjä, T., Koponen, I. S., and Paatero, P.: Evaluation of an automatic algorithm for fitting the particle number size distributions, *Boreal Environ. Res.*, 10, 337–355, 2005. 5812

Kalivitis, N., Birmili, W., Stock, M., Wehner, B., Massling, A., Wiedensohler, A., Gerasopoulos, E., and Mihalopoulos, N.: Particle size distributions in the Eastern Mediterranean troposphere, *Atmos. Chem. Phys.*, 8, 6729–6738, doi:10.5194/acp-8-6729-2008, 2008. 5809

15 Koulouri, E., Saarikoski, S., Theodosi, C., Markaki, Z., Gerasopoulos, E., Kouvarakis, G., Mäkelä, T., Hillamo, R., and Mihalopoulos, N.: Chemical composition and sources of fine and coarse aerosol particles in the Eastern Mediterranean, *Atmos. Environ.*, 42, 6542–6550, 2008. 5809

Knutson, E. O. and Whitby, K. T.: Aerosol classification by electric mobility: apparatus, theory, and applications, *J. Aerosol Sci.*, 6, 443–451, 1975. 5811

20 Kreidenweis, S. M., Petters, M. D., and DeMott, P. J.: Single parameter estimates of aerosol water content, *Environ. Res. Lett.*, 3, 035002, doi:10.1088/1748-9326/3/3/035002, 2008. 5815

Lelieveld, J., Berresheim, H., Borrmann, S., Crutzen, P. J., Dentener, F. J., Fisher, H., Feichter, J., Flatau, P. J., Heland, J., Holzinger, R., Kormann, R., Lawrence, M. G., Levin, Z., Markowitz, K. M., Mihalopoulos, N., Minikin, A., Ramanathan, V., de Reus, M., Roelofs, G. J., Scheeren, H. A., Sciare, J., Schlager, H., Schultz, M., Siegmund, P., Steil, B., Stephanou, E. G., Stier, P., Traub, M., Warneke, C., Williams, J., and Ziereis, H.: Global air pollution crossroads over the Mediterranean, *Science*, 298, 794–799, 2002. 5808

25 Liu, P. S.K., Deng, R., Smith, K. A., Williams, L. R., Jayne, J. T., Canagaratna, M. R., Moore, K., Onasch, T. B., Worsnop, D. R., and Deshler, T.: Transmission efficiency of an aerodynamic focusing lens system: comparison of model calculations and laboratory measurements for the Aerodyne Aerosol Mass Spectrometer, *Aerosol Sci. Tech.*, 41, 721–733, 2007. 5811

Aerosol particles  
over the Aegean Sea

S. Bezantakos et al.

Title Page

Abstract

Introduction

Conclusions

References

Tables

Figures

◀

▶

◀

▶

Back

Close

Full Screen / Esc

Printer-friendly Version

Interactive Discussion



- Marcolli, C., Luo, B. P., and Peter, T.: Mixing of the organic aerosol fractions: liquids as the thermodynamically stable phases, *J. Phys. Chem. A*, 108, 2216–2224, 2004. 5820
- Middlebrook, A. M., Bahreini, R., Jimenez, J. L., and Canagaratna, M. R.: Evaluation of composition-dependent collection efficiencies for the aerodyne aerosol mass spectrometer using field data, *Aerosol Sci. Tech.*, 46, 258–271, 2012. 5814
- 5 Mihalopoulos, N., Stephanou, E., Kanakidou, M., Pilitsidis, S., and Bousquet, P.: Tropospheric aerosol ionic composition above the Eastern Mediterranean Area, *Tellus B*, 49, 314–326, 1997. 5808
- Morgan, W. T., Allan, J. D., Bower, K. N., Highwood, E. J., Liu, D., McMeeking, G. R., Northway, M. J., Williams, P. I., Krejci, R., and Coe, H.: Airborne measurements of the spatial distribution of aerosol chemical composition across Europe and evolution of the organic fraction, *Atmos. Chem. Phys.*, 10, 4065–4083, doi:10.5194/acp-10-4065-2010, 2010. 5810
- 10 Ogren, J. and Charlson, J.: Implications for models and measurements of chemical inhomogeneities among cloud droplets, *Tellus B*, 44, 489–504, 1992. 5808
- 15 Park, K., Kim, J. S., and Miller, A. L.: A study on effects of size and structure on hygroscopicity of nanoparticles using a tandem differential mobility analyzer and TEM, *J. Nanopart. Res.*, 11, 175–183, 2009. 5819
- Petters, M. D. and Kreidenweis, S. M.: A single parameter representation of hygroscopic growth and cloud condensation nucleus activity, *Atmos. Chem. Phys.*, 7, 1961–1971, doi:10.5194/acp-7-1961-2007, 2007. 5808, 5815
- 20 Pikridas, M., Bougiatioti, A., Hildebrandt, L., Engelhart, G. J., Kostenidou, E., Mohr, C., Prévôt, A. S. H., Kouvarakis, G., Zarmas, P., Burkhardt, J. F., Lee, B.-H., Psychoudaki, M., Mihalopoulos, N., Pilinis, C., Stohl, A., Baltensperger, U., Kulmala, M., and Pandis, S. N.: The Finokalia Aerosol Measurement Experiment – 2008 (FAME-08): an overview, *Atmos. Chem. Phys.*, 10, 6793–6806, doi:10.5194/acp-10-6793-2010, 2010. 5809
- 25 Pilinis, C. and Seinfeld, J. H.: Continued development of a general equilibrium model for inorganic multicomponent atmospheric aerosols, *Atmos. Environ.*, 21, 2453–2466, 1987. 5815
- Rader, D. J. and McMurry P. H.: Application of the tandem differential mobility analyzer to studies of droplet growth or evaporation, *J. Aerosol Sci.* 17, 771–787, 1986. 5811
- 30 Salisbury, G., Williams, J., Holzinger, R., Gros, V., Mihalopoulos, N., Vrekoussis, M., Sarda-Estève, R., Berresheim, H., von Kuhlmann, R., Lawrence, M., and Lelieveld, J.: Ground-based PTR-MS measurements of reactive organic compounds during the MINOS campaign

Aerosol particles  
over the Aegean Sea

S. Bezantakos et al.

Title Page

Abstract

Introduction

Conclusions

References

Tables

Figures

◀

▶

◀

▶

Back

Close

Full Screen / Esc

Printer-friendly Version

Interactive Discussion



in Crete, July–August 2001, Atmos. Chem. Phys., 3, 925–940, doi:10.5194/acp-3-925-2003, 2003. 5809

Spengler, J. D., Brauer, M., and Koutrakis, P.: Acid air and health, Environ. Sci. Technol., 24, 946–955, 1990. 5822

5 Stock, M., Cheng, Y. F., Birmili, W., Massling, A., Wehner, B., Müller, T., Leinert, S., Kalivitis, N., Mihalopoulos, N., and Wiedensohler, A.: Hygroscopic properties of atmospheric aerosol particles over the Eastern Mediterranean: implications for regional direct radiative forcing under clean and polluted conditions, Atmos. Chem. Phys., 11, 4251–4271, doi:10.5194/acp-11-4251-2011, 2011. 5809, 5819

10 Stolzenburg, M. R. and McMurry, P. H.: TDMAFIT User's Manual, Particle Technology Laboratory, Department of Mechanical Engineering, University of Minnesota, Minneapolis, 1–61, 1988. 5814

Stolzenburg, M. R. and McMurry, P. H.: An ultrafine aerosol Condensation Nucleus Counter, Aerosol Sci. Tech., 14, 48–65, 1991. 5811

15 Tombrou, M., Bossioli, E., Kalogiros, J., Allan, J., Bacak, A., Biskos, G., Coe, H., Dandou, A., Kouvarakis, G., Mihalopoulos, N., Protonotariou, A. P., Szabó-Takács, B., and Triantafyllou, E.: Physical and Chemical Processes of Polluted Air Masses During Etesians: Aegean-Game Airborne Campaign – An Outline, in Advances in Meteorology, Climatology and Atmospheric Physics, Springer Atmospheric Sciences, 1239–1244, Springer-Verlag Berlin Heidelberg, doi:10.1007/978-3-642-29172-2\_173, 2012. 5810

20 Wang, C. S. and Flagan C. R.: Scanning electrical mobility spectrometer, Aerosol Sci. Tech., 13, 230–240, 1989. 5811

Wang, X., Kruis, F. E., and McMurry, P. H.: Aerodynamic focusing of nanoparticles: I. Guidelines for designing aerodynamic lenses for nanoparticles, Aerosol Sci. Tech., 39, 611–623, 2005.

25 5811

Aerosol particles  
over the Aegean Sea

S. Bezantakos et al.

Title Page

Abstract

Introduction

Conclusions

References

Tables

Figures

◀

▶

◀

▶

Back

Close

Full Screen / Esc

Printer-friendly Version

Interactive Discussion

**Table 1.** Hygroscopic parameters  $\kappa$  and densities  $\rho$  used in the  $\kappa$ -Köhler theory (Eq. 3).

Chemical species	$\kappa$	$\rho$ (kgm <sup>-3</sup> )
(NH <sub>4</sub> ) <sub>2</sub> SO <sub>4</sub>	0.53	1769
NH <sub>4</sub> HSO <sub>4</sub>	0.56	1720
NH <sub>4</sub> NO <sub>3</sub>	0.68	1780
H <sub>2</sub> SO <sub>4</sub>	1.19	1830
Organics	0.00–0.20	1200–1700

Aerosol particles  
over the Aegean Sea

S. Bezantakos et al.

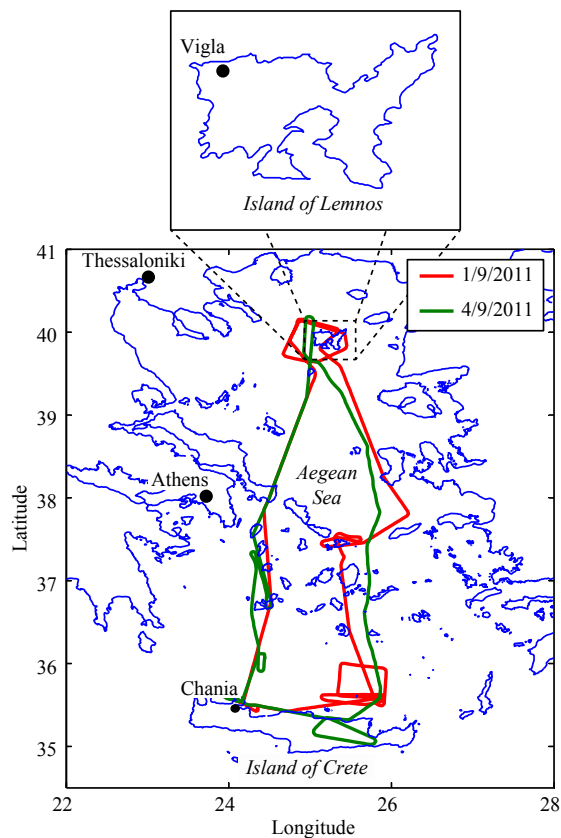


**Fig. 1.** Map of Greece showing the island of Lemnos, and the location of the ground station at Vigla on the northwestern part of the island. The red and green light show the flight paths followed by the FAAM BAe-146 aircraft on 1 and 4 September, respectively.

Title Page

Abstract

Introduction

Conclusions

References

Tables

Figures

◀

▶

◀

▶

Back

Close

Full Screen / Esc

Printer-friendly Version

Interactive Discussion



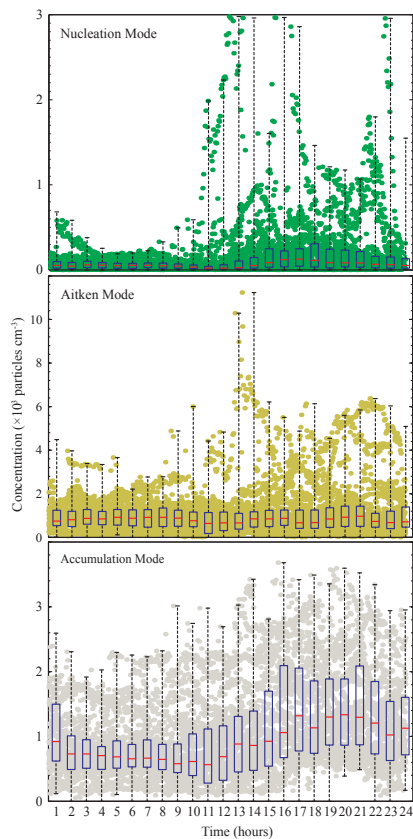


**Fig. 2.** Total number concentration of nucleation-mode (top), Aitken-mode (middle) and accumulation-mode (bottom) particles at the ground station on Lemnos. Red lines represent the hourly median values, boxes the 25th and 75th percentiles and whiskers the minimum and maximum values.

Title Page	
Abstract	Introduction
Conclusions	References
Tables	Figures
◀	▶
◀	▶
Back	Close
Full Screen / Esc	
Printer-friendly Version	
Interactive Discussion	



Aerosol particles  
over the Aegean Sea

S. Bezantakos et al.

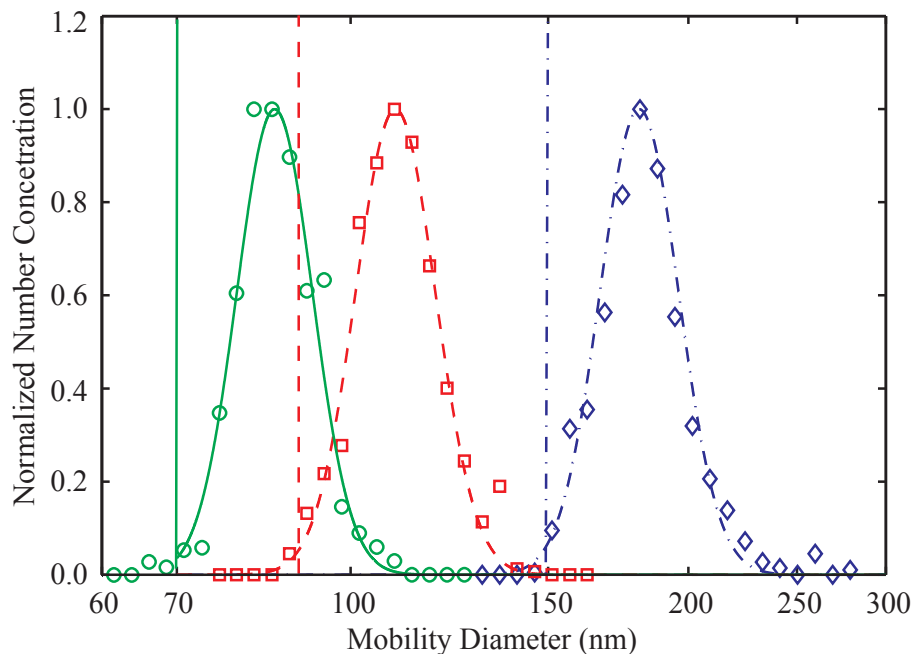


**Fig. 3.** Size distribution measurements of the humidified monodisperse-particle samples recorded by the HTDMA system. Particles having dry mobility diameters of 70 (green), 90 (red), and 150 nm (blue) selected by DMA-1 at ca. 30% RH were exposed to 85% RH and measured by DMA-2 and the CPC. Symbols represent the actual measurements and lines the fitted curves determined by the inversion algorithm. One hygroscopic mode is observed in all the measurements, corresponding to growth factors of 1.22, 1.22 and 1.21, for the 70-, 90- and 150-nm dry particles, respectively.

[Title Page](#)[Abstract](#)[Introduction](#)[Conclusions](#)[References](#)[Tables](#)[Figures](#)[◀](#)[▶](#)[◀](#)[▶](#)[Back](#)[Close](#)[Full Screen / Esc](#)[Printer-friendly Version](#)[Interactive Discussion](#)

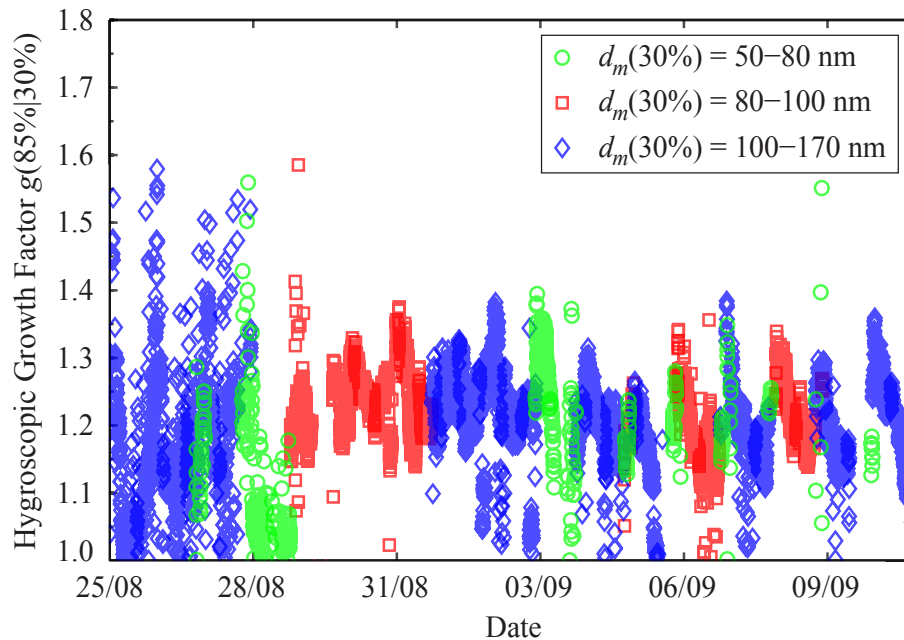


**Fig. 4.** Time series of hygroscopic growth factors of atmospheric aerosol particles measured with the HTDMA on the ground station on Lemnos from 25 August to 10 September 2011. Aerosol particles were grouped in three different regions based on their dry mobility diameters: from 50 to 80 nm (green circles), from 80 to 100 nm (red squares), and from 100 to 170 nm (blue diamonds).

Title Page	
Abstract	Introduction
Conclusions	References
Tables	Figures
◀	▶
◀	▶
Back	Close
Full Screen / Esc	
Printer-friendly Version	
Interactive Discussion	



Aerosol particles  
over the Aegean Sea

S. Bezantakos et al.

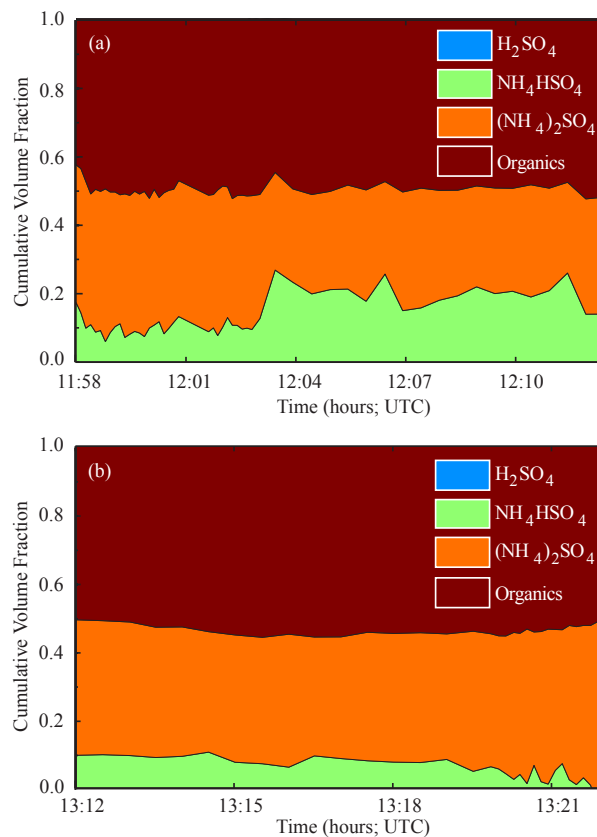


**Fig. 5.** Cumulative volume fractions of chemical species comprising the particles in the atmosphere over the ground station on 1 (a) and 4 (b) September 2011. The volume fractions are estimated by applying the ion pairing algorithm to the chemical composition measurements from the airborne cTOF-AMS.

[Title Page](#)[Abstract](#)[Introduction](#)[Conclusions](#)[References](#)[Tables](#)[Figures](#)[◀](#)[▶](#)[◀](#)[▶](#)[Back](#)[Close](#)[Full Screen / Esc](#)[Printer-friendly Version](#)[Interactive Discussion](#)

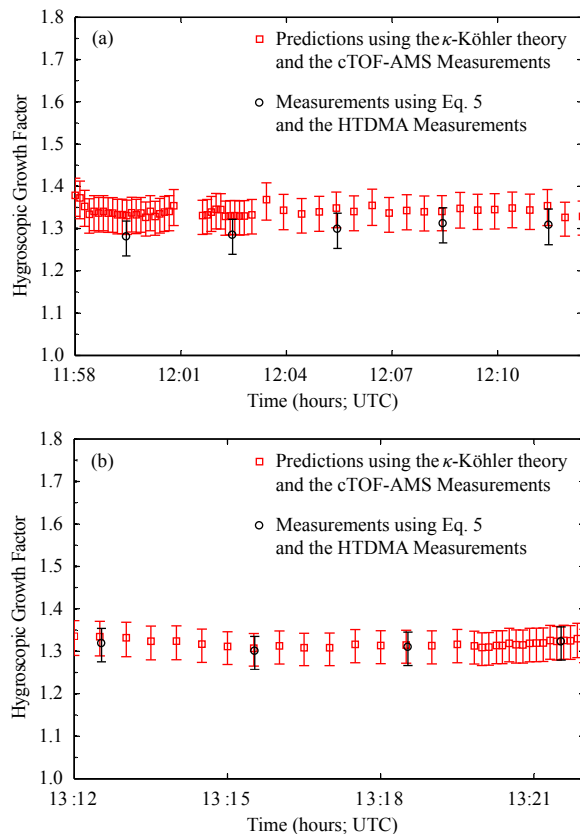


**Fig. 6.** Hygroscopic growth factors measured by the HTDMA (black dots) and predicted by  $\kappa$ -Köhler theory using the chemical composition measurements from the airborne cTOF-AMS (red squares) when the aircraft was flying close to Vigla station on 1 (a) and 4 (b) September 2011. The HTDMA growth factors correspond to particles having dry mobility diameter of 100 nm, whereas the chemical composition corresponds to particles having diameter in the range 50–700 nm. Error bars represent the 2% uncertainty in the RH measurements.

[Title Page](#)[Abstract](#)[Introduction](#)[Conclusions](#)[References](#)[Tables](#)[Figures](#)[◀](#)[▶](#)[◀](#)[▶](#)[Back](#)[Close](#)[Full Screen / Esc](#)[Printer-friendly Version](#)[Interactive Discussion](#)

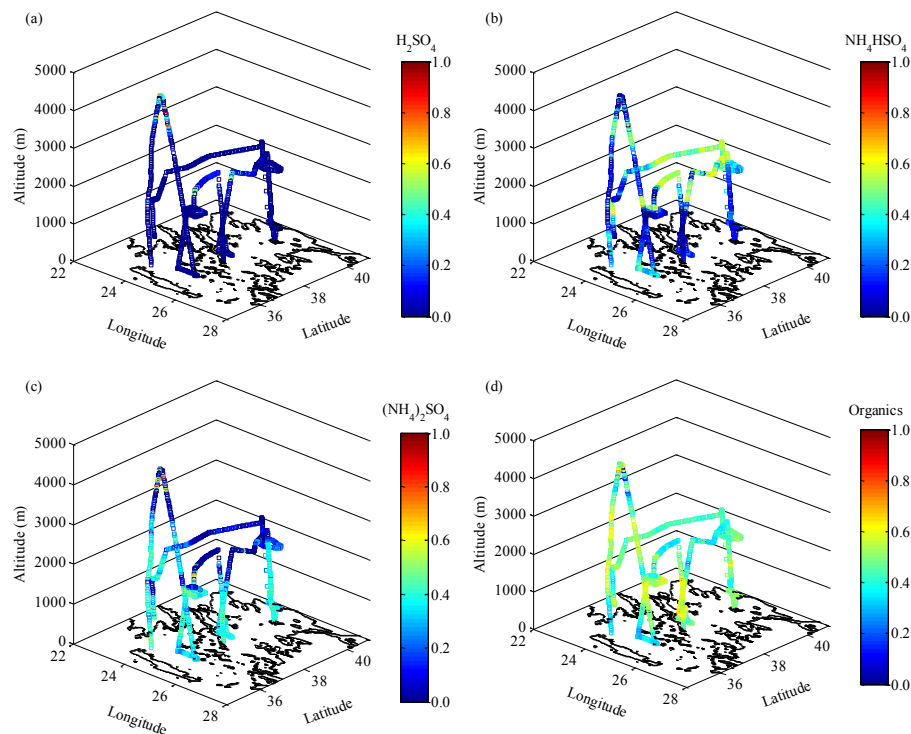


**Fig. 7.** Composition of the non-refractory compounds measured by the cTOF-AMS during the entire flight over the Aegean Sea on 1 September 2011. The reported volume fractions for  $\text{H}_2\text{SO}_4$  (a),  $\text{NH}_4\text{HSO}_4$  (b),  $(\text{NH}_4)_2\text{SO}_4$  (c) and organic matter (d) are estimated using the mole fractions determined by the cTOF-AMS measurements and the simplified ion pairing algorithm proposed by Gysel et al. (2007).

[Title Page](#)[Abstract](#)[Introduction](#)[Conclusions](#)[References](#)[Tables](#)[Figures](#)[◀](#)[▶](#)[◀](#)[▶](#)[Back](#)[Close](#)[Full Screen / Esc](#)[Printer-friendly Version](#)[Interactive Discussion](#)

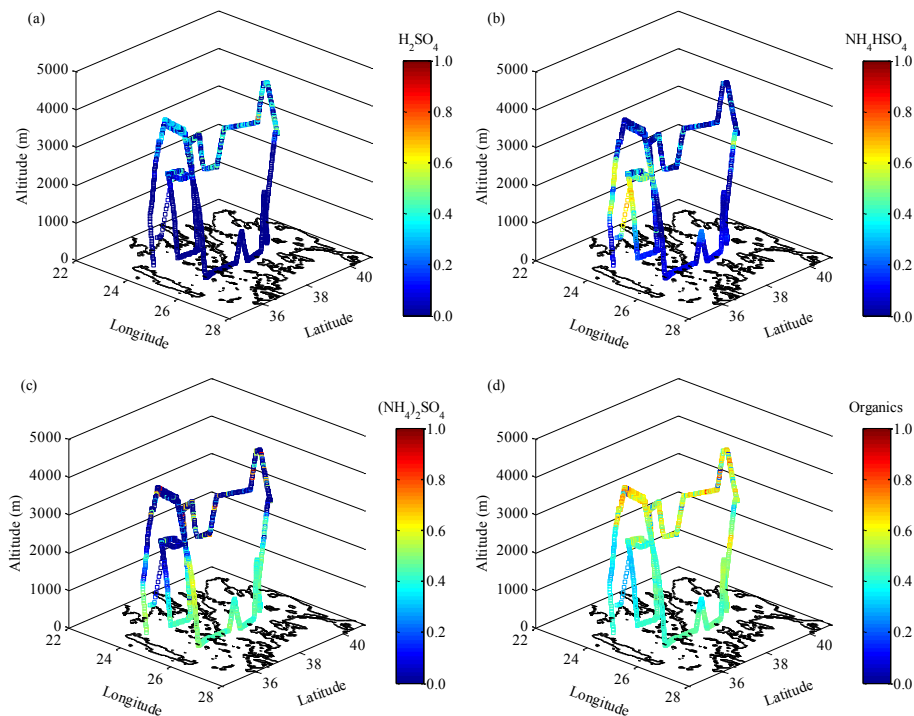


**Fig. 8.** Composition of the non-refractory compounds measured by the cTOF-AMS during the entire flight over the Aegean Sea on 4 September 2011. The reported volume fractions for  $\text{H}_2\text{SO}_4$  (a),  $\text{NH}_4\text{HSO}_4$  (b),  $(\text{NH}_4)_2\text{SO}_4$  (c) and organic matter (d) are estimated using the mole fractions determined by the cTOF-AMS measurements and the simplified ion pairing algorithm proposed by Gysel et al. (2007).

[Title Page](#)[Abstract](#)[Introduction](#)[Conclusions](#)[References](#)[Tables](#)[Figures](#)[◀](#)[▶](#)[◀](#)[▶](#)[Back](#)[Close](#)[Full Screen / Esc](#)[Printer-friendly Version](#)[Interactive Discussion](#)

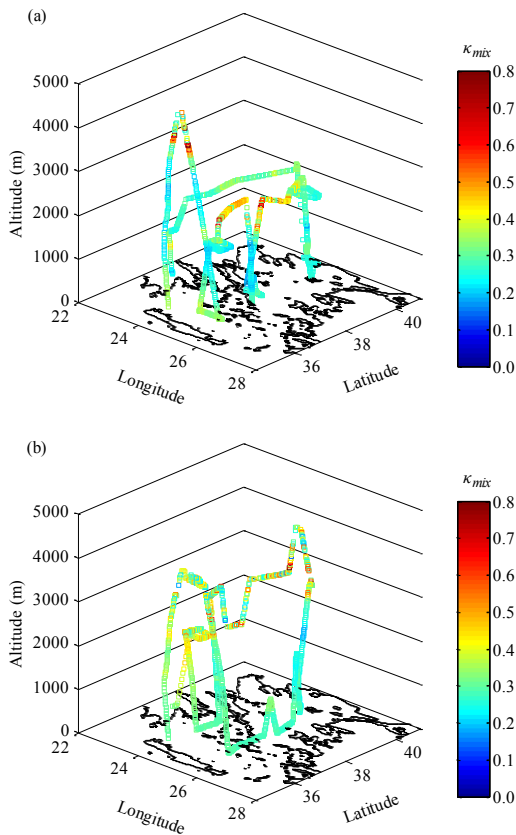


**Fig. 9.** Estimated hygroscopic parameters  $\kappa_{\text{mix}}$  of aerosol particles observed over the Aegean Sea on 1 **(a)** and 4 **(b)** of September 2011. The hygroscopic parameters are calculated using the  $\kappa$ -Köhler theory (Eq. 3) and the chemical composition measurements from the airborne cTOF-AMS. For the calculations we assumed that the particles were internally mixed, and that all the organic species were hydrophobic, i.e.  $\kappa_{\text{org}} = 0$ .